

This article was downloaded by:
On: 25 January 2011
Access details: Access Details: Free Access
Publisher *Taylor & Francis*
Informa Ltd Registered in England and Wales Registered Number: 1072954 Registered office: Mortimer House, 37-41 Mortimer Street, London W1T 3JH, UK



Separation Science and Technology

Publication details, including instructions for authors and subscription information:

<http://www.informaworld.com/smpp/title~content=t713708471>

Effects of Inclined Angle and Aspect Ratio on Heavy Water Separation Efficiencies in Double-Flow Thermal-Diffusion Columns with External Refluxes

Chii-Dong Ho^a; Hsuan Chang^a; Jia-Jan Guo^a

^a Department of Chemical and Materials Engineering, Tamkang University, Tamsui, Taipei, R.O.C.

Online publication date: 08 July 2010

To cite this Article Ho, Chii-Dong , Chang, Hsuan and Guo, Jia-Jan(2005) 'Effects of Inclined Angle and Aspect Ratio on Heavy Water Separation Efficiencies in Double-Flow Thermal-Diffusion Columns with External Refluxes', Separation Science and Technology, 39: 5, 975 — 1004

To link to this Article: DOI: 10.1081/SS-120028565

URL: <http://dx.doi.org/10.1081/SS-120028565>

PLEASE SCROLL DOWN FOR ARTICLE

Full terms and conditions of use: <http://www.informaworld.com/terms-and-conditions-of-access.pdf>

This article may be used for research, teaching and private study purposes. Any substantial or systematic reproduction, re-distribution, re-selling, loan or sub-licensing, systematic supply or distribution in any form to anyone is expressly forbidden.

The publisher does not give any warranty express or implied or make any representation that the contents will be complete or accurate or up to date. The accuracy of any instructions, formulae and drug doses should be independently verified with primary sources. The publisher shall not be liable for any loss, actions, claims, proceedings, demand or costs or damages whatsoever or howsoever caused arising directly or indirectly in connection with or arising out of the use of this material.

Effects of Inclined Angle and Aspect Ratio on Heavy Water Separation Efficiencies in Double-Flow Thermal-Diffusion Columns with External Refluxes

Chii-Dong Ho,* Hsuan Chang, and Jia-Jan Guo

Department of Chemical and Materials Engineering, Tamkang
University, Tamsui, Taipei, Taiwan, R.O.C.

ABSTRACT

The heavy water separation efficiency enhancement in double-flow, by inserting an impermeable sheet or a permeable barrier into double-flow thermal-diffusion columns with external refluxes at the ends has been investigated analytically. The analysis is conducted when using an orthogonal expansion technique. The separation efficiencies are compared with conventional Clusius–Dickel columns of the same size. Considerable improvements in heavy water enrichment in double-flow thermal-diffusion columns can be obtained by increasing the inclined angle and/or by decreasing the aspect ratio. Analytical results also show

*Correspondence: Professor Chii-Dong Ho, Department of Chemical and Materials Engineering, Tamkang University, Tamsui, Taipei 251, R.O.C.; Fax: 886-2-26209887; E-mail: cdho@mail.tku.edu.tw.

that both the recycle ratio and the position of insertion are important design parameters.

Key Words: Water isotopes; Orthogonal expansion techniques; Inclined angle; Aspect ratio; Thermal diffusion.

INTRODUCTION

The transport phenomenon of thermal diffusion was first discovered by Enskog^[1] in 1911 from theoretical considerations of the kinetic theory of a gas mixture and was later demonstrated experimentally by Chapman and Dootson^[2] in 1917. In static systems, which were used in the early study on the thermal-diffusion effect, the temperature gradient was established in such a fashion that mass convection was eliminated by the concentration gradient flux due to ordinary diffusion and resulting in no net bulk flow. Subsequently, Clusius and Dickel^[3,4] pointed out that convective currents could be created to produce cascading effects, analogous to the multistage effect of countercurrent extraction and result in a considerable separation efficiency improvement. Applications of the convective-current concept in practical separation systems were presented and investigated by Furry et al.^[5,6] Recently, heavy water enrichment by using the Clusius–Dickel column was studied both theoretically and experimentally by Yeh et al.^[7–9]

Previous theoretical studies on the Clusius–Dickel column have indicated that the convective currents in the vertical thermal-diffusion columns actually have two conflicting effects, the advantageous cascading effect and the disadvantageous remixing effect on the mass diffusion along the column axially and across the column radially.^[3,4] Improved design, hence, can be obtained via the suppression of the remixing effect or the enhancement of the cascading effect. It has been shown that in a flat-plate column, the disadvantageous remixing effect can be effectively reduced and adjusted by using the inclined vertical column.^[10] Based on the concept of reducing convection strength, there have been many improved designs for the Clusius–Dickel column, including inclined columns,^[11,12] wired columns,^[13,14] inclined moving-wall columns,^[15,16] rotary columns,^[17–19] packed columns,^[20,21] rotary wired columns,^[22,23] permeable barrier columns,^[24,25] and impermeable barrier columns.^[26]

The introduction of recycling into double-pass parallel-plate mass exchangers has been proved to be capable of enhancing mass-transfer coefficients.^[27–29] The purpose of this study is to investigate the effects of the aspect ratio and the inclination angle on the performance of the Clusius–Dickel columns with recycling and insertion of an impermeable sheet or a permeable barrier. The transport phenomena in such devices belong to the category of conjugated Graetz

problems. The theoretical formulations of such conjugated Graetz problems were solved by using the orthogonal expansion technique.^[25,30-36] The improvements of the device performance of double-flow thermal-diffusion columns with external refluxes operated at various design and parameters are analyzed.

THEORETICAL FORMULATIONS

Inclined Clusius–Dickel Column

The transport equations for heavy water separation enrichment in the continuous Clusius–Dickel column, as shown in Fig. 1, have been developed

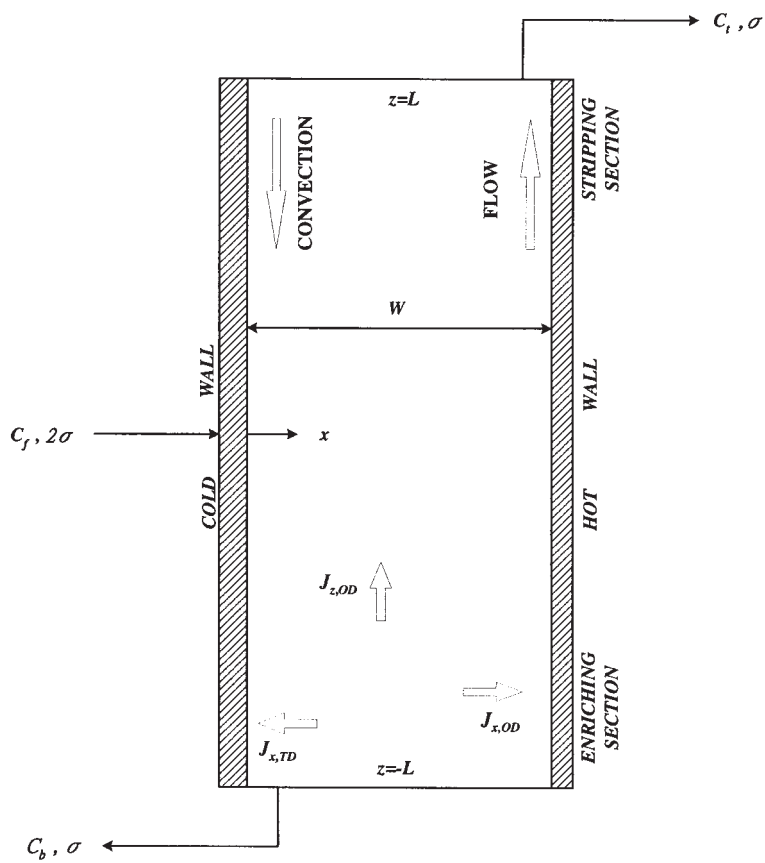


Figure 1. Schematic diagram of the continuous-type thermal-diffusion column.



in our previous work.^[29] The degree of separation of the entire column can be determined as follows

$$\Delta_0 = C_b - C_t = \Delta_e + \Delta_s = (F_e + F_s) \frac{1 - e^{-\sigma' L'/2}}{\sigma'} \quad (1)$$

where transport constants and the dimensionless variables are defined as

$$H = \frac{\alpha \beta \rho g (2\omega)^3 (\Delta T)^2}{6! \mu \bar{T}} < 0, \quad K = \frac{\rho g^2 \beta^2 W^7 B (\Delta T)^2}{9! \mu^2 D} \quad (2)$$

and

$$\sigma' = \frac{\sigma}{-H}, \quad L' = \frac{L(-H)}{K} \quad (3)$$

The pseudoconcentration product is defined as

$$C\hat{C} = C \left\{ 0.05263 - (0.05263 - 0.0135K_{eq})C - 0.027 \left\{ \left[1 - \left(1 - \frac{K_{eq}}{4} \right) C \right] CK_{eq} \right\}^{1/2} \right\} \quad (4)$$

in which

$$K_{eq} = \frac{[HDO]^2}{[H_2O][D_2O]} \times \frac{19 \times 19}{18 \times 20} \quad (5)$$

In Eq. (1), F_e and F_s are defined as

$$F_e = C_e \hat{C}_e = \frac{1}{C_B - C_F} \int_{C_F}^{C_B} C \hat{C} dC \quad (6)$$

$$F_s = C_s \hat{C}_s = \frac{1}{C_F - C_T} \int_{C_T}^{C_F} C \hat{C} dC \quad (7)$$

A simple and adaptable way of reducing the convective strength is to incline a flat-plate column with the hot plate on top, so as to diminish the effective gravitational force. The separation equations for an inclined



column can be obtained easily by replacing g with $g\cos\phi$ in Eq. (2), that is,

$$H' = \frac{\alpha\beta\rho\cos\phi g(2\omega)^3(\Delta T)^2}{6!\mu\tilde{T}} = H\cos\phi \quad (8a)$$

$$K' = \frac{\rho g^2\cos^2\phi\beta^2W^7B(\Delta T)^2}{9!\mu^2D} = K\cos^2\phi \quad (8b)$$

The degree of separation in an inclined Clusius–Dickel column can be determined using by Eqs. (1), (3), (4), (8a), and (8b).

Inclined Clusius–Dickel Column with External Refluxes

A new design of continuous-type thermal diffusion columns inserts an impermeable sheet or a permeable barrier between the plates, as shown in Figs. 2 and 3, is proposed. The column is composed of enriching and stripping sections. The channel thickness of two sections are W_A and W_B , respectively. Feed enters from the center of the column and output products can be drawn from both ends.

In obtaining the theoretical formulation, the following assumptions are made: (a) heat transfer between the space of the hot and cold plates is by conduction only; (b) fluid flow is purely laminar; (c) the influences of ordinary and thermal diffusions, end effects, and inertia terms on the velocity are neglected; (d) ordinary diffusion in the vertical direction and bulk flow in the horizontal direction are neglected; and (e) fluxes due to thermal diffusion are constant (i.e., $\alpha\hat{C}C/\tilde{T}$, $\alpha C_{Ae}\hat{C}_{Ae}/\tilde{T}$, and $\alpha C_{Be}\hat{C}_{Be}/\tilde{T}$ are constant and equal to θ). For the inclined column with the insertion of a permeable barrier or an impermeable sheet in the enriching section, the following dimensionless variables are introduced:

$$\begin{aligned} \eta_A &= \frac{x_A}{W_A}, \quad \eta_B = \frac{x_B}{W_B}, \quad s = \frac{z}{L}, \\ \tilde{T} &= \frac{2W_A^3T_1 + 2W_B^3T_2 - h_1(W_A^4 - W_B^2)}{2(W_A^3 + W_B^2)} \\ h_1 &= \frac{\Delta T}{W_A + W_B + (k_f\delta)/[k_f\varepsilon + k(1 - \varepsilon)]}, \\ h_2 &= \frac{h_1k_f}{k_f\varepsilon + k(1 - \varepsilon)}, \quad \kappa = \frac{W_A}{W}, \quad R = \frac{\sigma_R}{\sigma} \end{aligned} \quad (9)$$

where h_1 is the temperature gradient of the fluid between hot and cold plates, and h_2 is the temperature gradient of the fluid within the barrier.



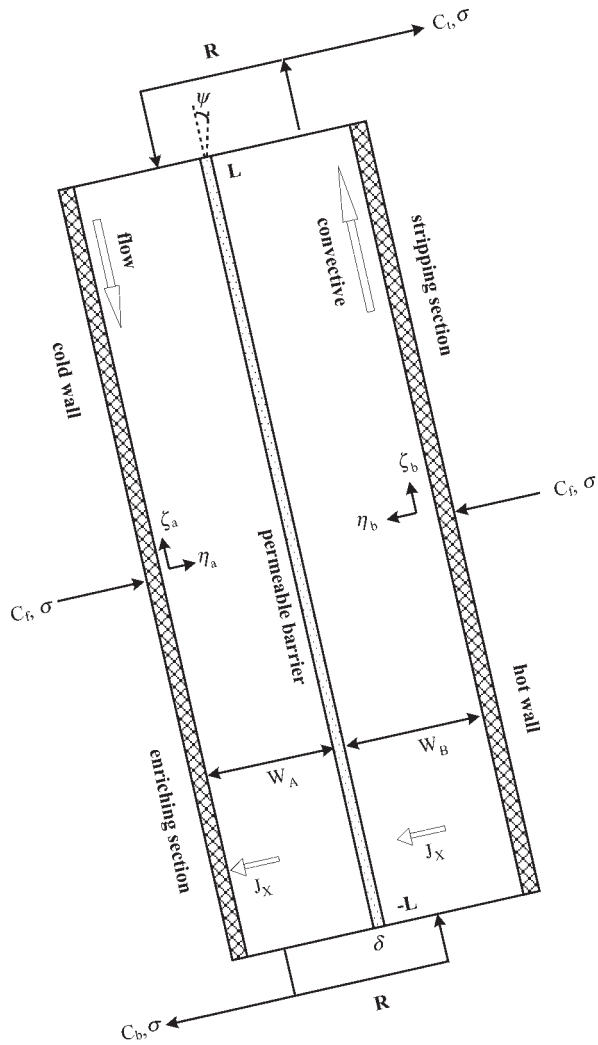


Figure 2. Schematic diagram of a double-flow inclined thermal-diffusion column with a vertical permeable barrier inserted.



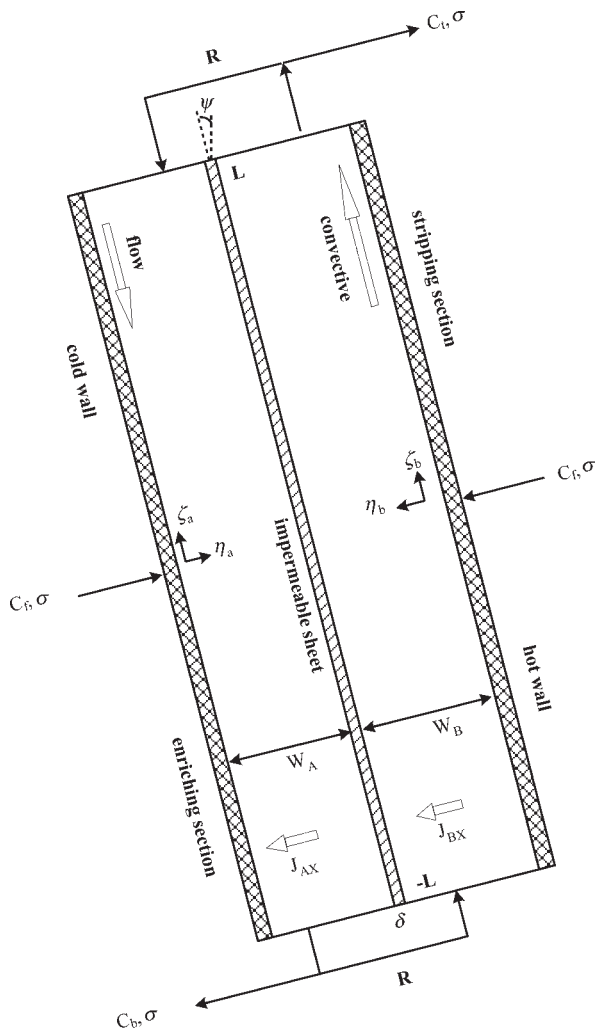


Figure 3. Schematic diagram of a double-flow inclined thermal-diffusion column with a vertical impermeable sheet inserted.

The velocity distribution in dimensionless form for the enriching section may be written as

$$V_{Ae}(\eta_A) = -f_{1e}(\eta_A - \eta_A^3) + f_{2e}(\eta_A^2 - \eta_A) + (1 + R)f_{3e}(\eta_A - \eta_A^2) \quad (10)$$

$$V_{Be}(\eta_B) = g_{1e}(\eta_B - \eta_B^3) - g_{2e}(\eta_B^2 - \eta_B) + Rg_{3e}(\eta_B - \eta_B^2) \quad (11)$$



in which

$$\begin{aligned}
 f_{1e} &= \frac{\beta g \cos \phi h_1 W_A^3}{6\mu}, \quad f_{2e} = \frac{\beta g \cos \phi W_A^2 [2W_B^3 \Delta T - h_1 (W_A^4 - W_B^4)]}{4\mu (W_A^3 + W_B^3)} \\
 f_{3e} &= \frac{6W_A^2 \sigma}{\rho B (W_A^3 + W_B^3)}, \quad g_{1e} = \frac{\beta g \cos \phi h_1 W_B^3}{6\mu} \\
 g_{2e} &= \frac{\beta g \cos \phi W_B^2 [2W_A^3 \Delta T + h_1 (W_B^4 - W_A^4)]}{4\mu (W_A^3 + W_B^3)}, \quad g_{3e} = \frac{6W_B^2 \sigma}{\rho B (W_A^3 + W_B^3)}
 \end{aligned} \tag{12}$$

For the stripping section, all these equations are still valid except that the subscript "e" must be replaced by "s" and R in Eq. (11), and $(1 + R)$ in Eq. (10) should be replaced by $(1 + R)$ and R , respectively.

(A) A Permeable Barrier Inserted

For the double-pass continuous-type thermal diffusion column with the permeable barrier inserted between the plates, as shown in Fig. 2, the equations of mass transfer for each slit in the enriching section in dimensionless form are

$$\frac{\partial^2 C_{Ae}}{\partial \eta_A^2} = \left(\frac{W_A^2 V_{Ae}}{LD} \right) \frac{\partial C_{Ae}}{\partial \zeta} \tag{13}$$

$$\frac{\partial^2 C_{Be}}{\partial \eta_B^2} = \left(\frac{W_B^2 V_{Be}}{LD} \right) \frac{\partial C_{Be}}{\partial \zeta} \tag{14}$$

The thermal diffusion term has been eliminated in both Eqs. (13) and (14) because of the assumption (e). The associated boundary conditions are

$$\frac{-\partial C_{Ae}}{\partial \eta_A} + \alpha \theta h_1 W_A = 0 \quad \text{at } \eta_A = 0 \tag{15}$$

$$\frac{\partial C_{Be}}{\partial \eta_B} + \alpha \theta h_1 W_B = 0 \quad \text{at } \eta_B = 0 \tag{16}$$

$$\frac{-\partial C_{Ae}}{\partial \eta_A} + \alpha \theta h_1 W_A = \frac{W_A}{W_B} \left[\frac{\partial C_{Be}}{\partial \eta_B} + \alpha \theta h_1 W_B \right] \quad \text{at } \eta_A = \eta_B = 1 \tag{17}$$

$$\begin{aligned}
 -\frac{\partial C_{Ae}}{\partial \eta_A} + \alpha \theta h_1 W_A \\
 = \frac{W_A \varepsilon}{\delta} \left[\alpha \theta h_2 \delta - \frac{C_{Be}}{D} + \frac{C_{Ae}}{D} \right] \quad \text{at } \eta_A = \eta_B = 1
 \end{aligned} \tag{18}$$

$$C_{Ae} = C_{Be} = C_t, \quad \text{at } \zeta = 1 \tag{19}$$



where α is the thermal diffusion constant. Equations (15) and (16) describe the continuity of mass fluxes on the impermeable hot and cold plates, whereas Eqs. (17) and (18) are for the two sides of the permeable barrier. Since it is imperative to have a mixing zone at the ends, Eq. (19) is imposed. For the stripping section, Eqs. (13)–(19) are still valid except that the symbol σ and subscript e should be replaced by $-\sigma$ and s, respectively.

The analytical solution to this type of problem can be obtained by using an orthogonal expansion technique. Separation of variables results in the following forms:

$$C_{Ae}(\eta_A, \zeta) = \theta h_1 W_A \eta_A + \sum_{m=0}^{\infty} S_{Ae,m} F_{Ae,m}(\eta_A) G_{e,m}(\zeta) \quad (20)$$

$$C_{Be}(\eta_B, \zeta) = -\theta h_1 W_B \eta_B + \sum_{m=0}^{\infty} S_{Be,m} F_{Be,m}(\eta_B) G_{e,m}(\zeta) + \theta(\Delta T) \quad (21)$$

Without losing generality, we may assume the eigenfunctions $F_{Ae,m}(\eta_A)$ and $F_{Be,m}(\eta_B)$ to be polynomials and can express them in the following forms:

$$F_{Ae,m}(\eta_A) = \sum_{n=0}^{\infty} d_{mn} \eta_A^n, \quad d_{m0} = 1 \text{ (selected)}, \quad d_{m1} = 0 \quad (22)$$

$$F_{Be,m}(\eta_B) = \sum_{n=0}^{\infty} e_{mn} \eta_B^n, \quad e_{m0} = 1 \text{ (selected)}, \quad e_{m1} = 0 \quad (23)$$

All the coefficients d_{mn} and e_{mn} may be expressed in terms of eigenvalue λ_m .

$$\begin{aligned} d_{m2} &= 0 \\ d_{m3} &= \frac{(1+R)\lambda_m W_A^2}{6LD} a_1 \\ d_{m4} &= \frac{(1+R)\lambda_m W_A^2}{12LD} a_2 \\ d_{m5} &= \frac{(1+R)\lambda_m W_A^2}{20LD} a_3 \\ d_{m(n+2)} &= \frac{(1+R)\lambda_m W_A^2}{(n+2)(n+1)LD} \\ &\quad \times [a_1 d_{m(n-1)} + a_2 d_{m(n-2)} + a_3 d_{m(n-3)}], \quad n \geq 4 \end{aligned} \quad (24)$$



and

$$\begin{aligned}
 e_{m2} &= 0 \\
 e_{m3} &= \frac{R\lambda_m W_B^2}{6LD} b_1 \\
 e_{m4} &= \frac{R\lambda_m W_B^2}{12LD} b_2 \\
 e_{m5} &= \frac{R\lambda_m W_B^2}{20LD} b_3 \\
 e_{m(n+2)} &= \frac{R\lambda_m W_B^2}{(n+2)(n+1)LD} \\
 &\quad \times [b_1 e_{m(n-1)} + b_2 e_{m(n-2)} + b_3 e_{m(n-3)}], \quad n \geq 4
 \end{aligned} \tag{25}$$

By following the same mathematical treatment performed in the previous work,^[26-28] the degree of separation for the whole column can be obtained by using the separation of variables method. Solving Eqs. (13) and (14) analytically with boundary conditions, Eqs. (15)-(19), and combining the concentration distributions in the enriching section give the general expressions for the expansion coefficients ($S_{Ac,m}$, $S_{Be,m}$, $S_{As,m}$, and $S_{Bs,m}$) in the stripping section as

$$\begin{aligned}
 &W_B \int_0^1 [C_t - \theta h_1 W_A \eta_A] \cdot \left[\frac{W_A^2 V_A(\eta_A)}{LD} \right] S_{As,m} F_{As,m} d\eta_A \\
 &\quad + W_A \int_0^1 [C_t + \theta h_1 W_B \eta_B] \cdot \left[\frac{W_B^2 V_A(\eta_A)}{LD} \right] S_{Bs,m} F_{Bs,m} d\eta_B \\
 &= W_B \int_0^1 S_{As,m}^2 \left[\frac{W_A^2 V_A(\eta_A)}{LD} \right] F_{As,m}^2 d\eta_A \\
 &\quad + W_A \int_0^1 S_{Bs,m}^2 \left[\frac{W_B^2 V_B(\eta_B)}{LD} \right] F_{Bs,m}^2 d\eta_B
 \end{aligned} \tag{26}$$

The average concentration differences for both channels A and B in the stripping section are obtained from Eqs. (27) and (28), respectively.

$$\begin{aligned}
 C_t - \frac{\int_0^1 V_{As}(\eta_A) C_{As}(\eta_A, 0) d\eta_A}{\int_0^1 V_{As}(\eta_B) d\eta_B} \\
 = \frac{DL \sum_{m=0, \lambda_{s,m}=0}^{\infty} [S_{As,m} F'_{As,m}(1) / \lambda_{s,m}] [\exp(\lambda_{s,m}) - 1]}{W_A^2 \int_0^1 V_{As}(\eta_A) d\eta_A}
 \end{aligned} \tag{27}$$



and

$$C_t - \frac{\int_0^1 V_{Bs}(\eta_B) C_{Bs}(\eta_B, 0) d\eta_B}{\int_0^1 V_{Bs}(\eta_B) d\eta_B} = \frac{DL \sum_{m=0, \lambda_{s,m}=0}^{\infty} [S_{Bs,m} F'_{Bs,m}(1)/\lambda_{s,m}] [\exp(\lambda_{s,m}) - 1]}{W_B^2 \int_0^1 V_{Bs}(\eta_B) d\eta_B} \quad (28)$$

In the enriching section, following the same procedure gives Eqs. (29) and (30) for channels A and B, respectively.

$$\frac{\int_0^1 V_{Ae}(\eta_A) C_{Ae}(\eta_A, 0) d\eta_A}{\int_0^1 V_{Ae}(\eta_A) d\eta_A} - C_b = \frac{DL \sum_{m=0, \lambda_{e,m}=0}^{\infty} [S_{Ae,m} F'_{Ae,m}(1)/\lambda_{e,m}] [1 - \exp(-\lambda_{e,m})]}{W_A^2 \int_0^1 V_{Ae}(\eta_A) d\eta_A} \quad (29)$$

and

$$\frac{\int_0^1 V_{Be}(\eta_B) C_{Be}(\eta_B, 0) d\eta_B}{\int_0^1 V_{Be}(\eta_B) d\eta_B} - C_b = \frac{DL \sum_{m=0, \lambda_{e,m}=0}^{\infty} [S_{Be,m} F'_{Be,m}(1)/\lambda_{s,m}] [1 - \exp(-\lambda_{e,m})]}{W_B^2 \int_0^1 V_{Be}(\eta_B) d\eta_B} \quad (30)$$

Combining Eqs. (27) and (29) [or Eqs. (28) and (30)] yields the degree of separation (Δ) for the whole column in terms of the eigenvalues ($\lambda_{e,m}$ and $\lambda_{s,m}$), expansion coefficients ($S_{Ae,m}$, $S_{Be,m}$, $S_{As,m}$, and $S_{Bs,m}$), permeable barrier position (κ), recycle ratio (R), and angle of inclination (ϕ). The analytical result is as follows

$$\Delta_m = C_b - C_t = \left(\frac{LD \sum_{m=0}^{\infty} [S_{Ae,m} F'_{Ae,m}(1)/\lambda_{e,m}] [1 - \exp(-\lambda_{e,m})]}{(\kappa W)^2 \int_0^1 V_{Ae} d\eta_A} + \frac{\int_0^1 V_{Ae} C_{Ae}(\eta_A, 0) d\eta_A}{\int_0^1 V_{Ae} d\eta_A} \right) - \left(\frac{\int_0^1 V_{As,m} C_{As}(\eta_A, 0) d\eta_A}{\int_0^1 V_{As} d\eta_A} - \frac{LD \sum_{m=0}^{\infty} [S_{As,m} F'_{As,m}(1)/\lambda_{s,m}] [\exp(\lambda_{s,m}) - 1]}{(\kappa W)^2 \int_0^1 V_{As} d\eta_A} \right) \quad (31)$$



or

$$\Delta_m = C_b - C_t = \left(\frac{LD \sum_{m=0}^{\infty} [S_{Be,m} F'_{Be,m}(1)/\lambda_{e,m}] [1 - \exp(-\lambda_{e,m})]}{(1 - \kappa)^2 W^2 \int_0^1 V_{Be} d\eta_B} \right. \\ \left. + \frac{\int_0^1 V_{Be} C_{Be}(\eta_B, 0) d\eta_B}{\int_0^1 V_{Be} d\eta_B} \right) - \left(\frac{\int_0^1 V_{Bs,m} C_{Bs}(\eta_B, 0) d\eta_B}{\int_0^1 V_{Bs} d\eta_B} \right. \\ \left. - \frac{LD \sum_{m=0}^{\infty} [S_{Bs,m} F'_{Bs,m}(1)/\lambda_{s,m}] [\exp(\lambda_{s,m}) - 1]}{(1 - \kappa)^2 W^2 \int_0^1 V_{Bs} d\eta_B} \right) \quad (32)$$

(B) An Impermeable Sheet Inserted

For the double-pass device with an impermeable sheet inserted, as shown in Fig. 3, a similar approach can be taken for deriving the equations. The equations of mass transfer for each slit in the enriching section also may be obtained in the same dimensionless form as in Eqs. (13) and (14), with the boundary conditions of Eqs. (17) and (18) being changed to

$$-\frac{\partial C_{Ae}}{\partial \eta_A} + \alpha \theta h_1 W_A = 0 \quad \text{at } \eta_A = 1 \quad (33)$$

$$\frac{\partial C_{Be}}{\partial \eta_B} + \alpha \theta h_1 W_B = 0 \quad \text{at } \eta_B = 1 \quad (34)$$

The two subchannels are separated by an impermeable sheet with negligible thermal resistance and, hence, share the temperature gradient. The calculation procedure is similar to that in the previous section, except the eigenvalues ($\lambda_{Ae,m}$, $\lambda_{As,m}$, and $\lambda_{Be,m}$, and $\lambda_{Bs,m}$) for each subchannel are calculated individually. The degree of separation for the double-pass device with an impermeable sheet inserted is

$$\Delta = C_b - C_t = \left(\frac{LD \sum_{m=0}^{\infty} [S_{Ae,m} F'_{Ae,m}(1)/\lambda_{Ae,m}] [1 - \exp(-\lambda_{Ae,m})]}{(\kappa W)^2 \int_0^1 V_{Ae} d\eta_A} \right. \\ \left. + \frac{\int_0^1 V_{Ae} C_{Ae}(\eta_A, 0) d\eta_A}{\int_0^1 V_{Ae} d\eta_A} \right) - \left(\frac{\int_0^1 V_{As,m} C_{As}(\eta_A, 0) d\eta_A}{\int_0^1 V_{As} d\eta_A} \right. \\ \left. - \frac{LD \sum_{m=0}^{\infty} [S_{As,m} F'_{As,m}(1)/\lambda_{As,m}] [\exp(\lambda_{As,m}) - 1]}{(\kappa W)^2 \int_0^1 V_{As} d\eta_A} \right) \quad (35)$$



or

$$\Delta = C_b - C_t = \left(\frac{LD \sum_{m=0}^{\infty} [S_{Be,m} F'_{Be,m}(1/\lambda_{Be,m})] [1 - \exp(-\lambda_{Be,m})]}{(1 - \kappa)^2 W^2 \int_0^1 V_{Be} d\eta_B} \right. \\ \left. + \frac{\int_0^1 V_{Be} C_{Be}(\eta_B, 0) d\eta_B}{\int_0^1 V_{Be} d\eta_B} \right) - \left(\frac{\int_0^1 V_{Bs,m} C_{Bs}(\eta_B, 0) d\eta_B}{\int_0^1 V_{Bs} d\eta_B} \right. \\ \left. - \frac{LD \sum_{m=0}^{\infty} [S_{Bs,m} F'_{Bs,m}(1/\lambda_{As,m})] [\exp(\lambda_{As,m}) - 1]}{(1 - \kappa)^2 W^2 \int_0^1 V_{Bs} d\eta_B} \right) \quad (36)$$

SEPARATION EFFICIENCY STUDY

The improvement of separation, I_m and I , for a permeable barrier and an impermeable sheet inserted, respectively, are defined relative to the vertical Clusius–Dickel column of the same size as

$$I_m = \frac{\Delta_m - \Delta_0}{\Delta_0} \quad (37)$$

and

$$I = \frac{\Delta - \Delta_0}{\Delta_0} \quad (38)$$

The ratio of column length to column width, the aspect ratio, is an important parameter affecting the separation efficiency in thermal diffusion columns. There are two parts needed to be included in the cost of using the thermal diffusion column: a fixed charge and an operation cost. The fixed charge depends on the equipment cost, while the main operating expense comes from the heat supply. If the temperature difference (ΔT) and thickness ($W_A + W_B$) between hot and cold walls are fixed, the total expenditure is determined when the plate-surface area (A) is specified. Hence, the effects of aspect ratio on the device performance for an inclined thermal-diffusion column with external refluxes is investigated for a given plate-surface area and are shown in Figs. 4 and 5.

RESULTS AND DISCUSSION

For illustration, a set of typical parameters is listed in Table 1. Tables 2 and 3 show the results of the first two eigenvalues and their associated



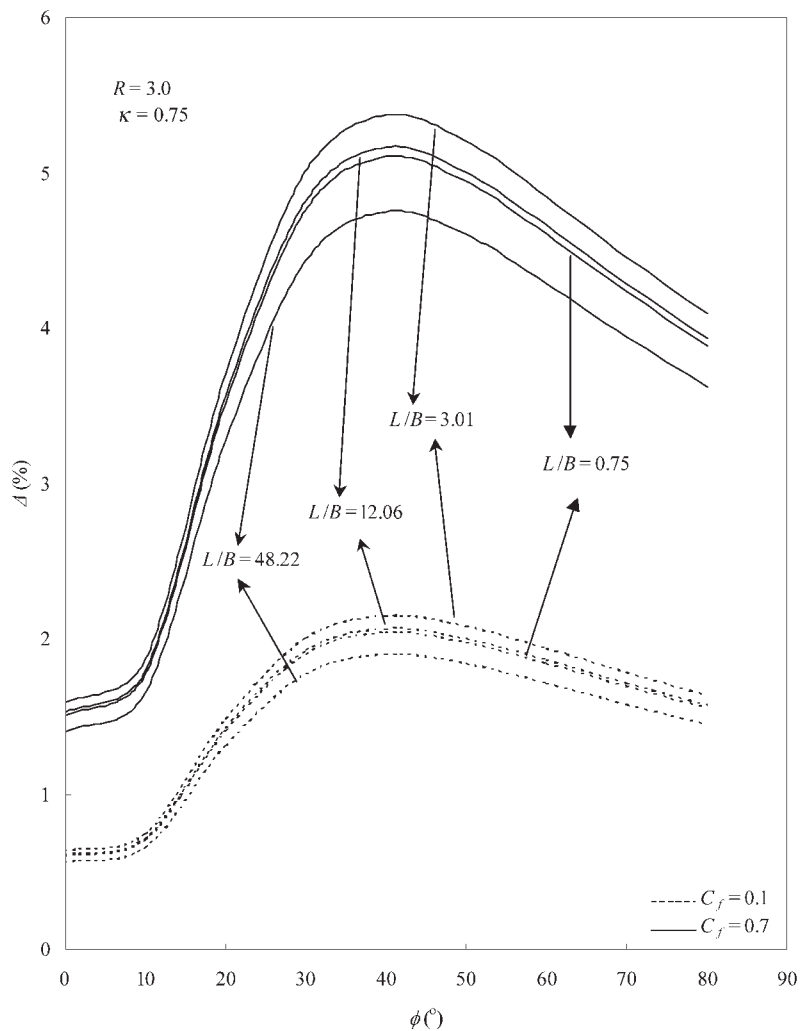


Figure 4. Effect of inclined angle for the column an impermeable sheet inserted on the degree of separation with aspect ratio as a parameter; $C_f = 0.1, 0.7$, $\sigma = 1.0$ g/hr, $R = 3.0$.



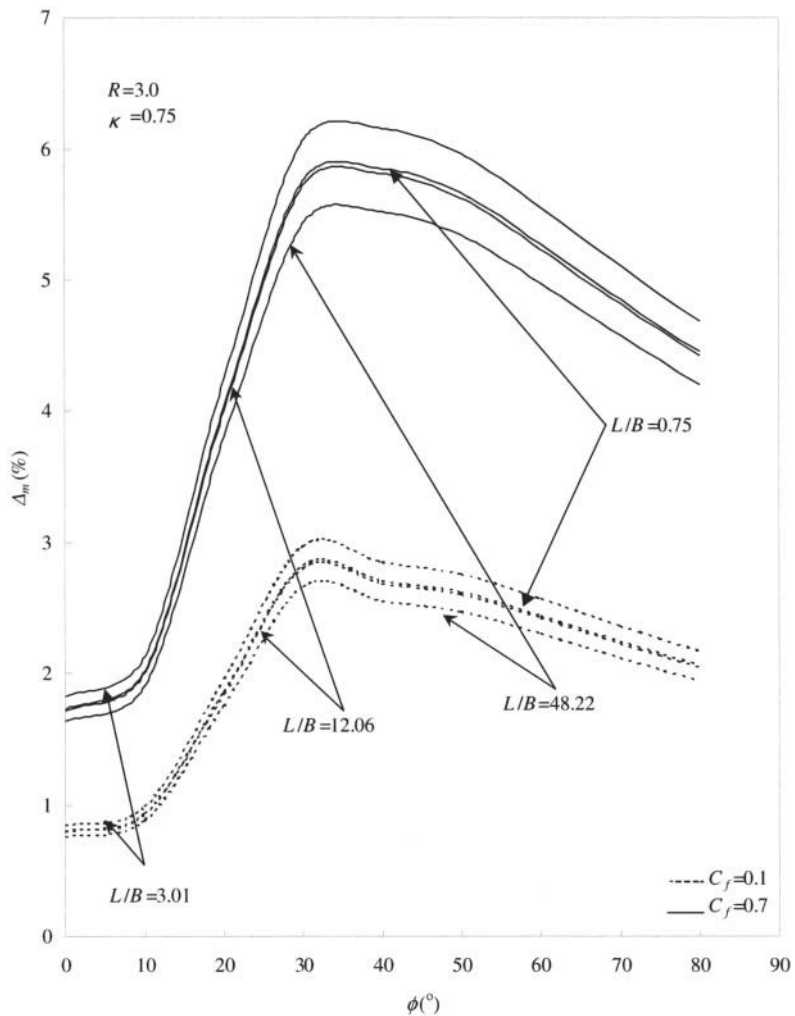


Figure 5. Effect of inclined angle for the column an permeable barrier inserted on the degree of separation with aspect ratio as a parameter; $C_f = 0.1, 0.7$, $\sigma = 1.0 \text{ g/hr}$, $R = 3.0$.

expansion coefficients for $R = 3.0$, $\kappa = 1/2$, $\sigma = 1.0 \text{ g/hr}$, and $C_f = 0.1$ for the inclined columns by inserting a permeable barrier and an impermeable sheet, respectively. Due to the rapid convergence characteristics, only the first negative eigenvalue is adopted for the calculation of the degree of separation.



Table 1. A set of typical parameters.

$B = 10.12 \text{ cm}$	$\beta = 5 \times 10^{-3} \text{ g/cm}^3 \text{ K}$
$\Delta T = 30.5 \text{ K}$	$D = 3.9 \times 10^{-5} \text{ cm}^2/\text{s}$
$L = 144 \text{ cm}$	$W_A + W_B = 0.08 \text{ cm}$
$\delta = 0.02 \text{ cm}$	$\alpha = -0.0184$
$\rho = 1.0 \text{ g/cm}^3$	$K_{\text{eq}} = 3.8$
$g = 980 \text{ cm/s}^2$	$\varepsilon = 0.378$
$\tilde{T} = 303.25 \text{ K}$	$A = 1457.28 \text{ cm}^2$
$\mu = 1.0 \text{ g/cm s}$	
$k_f = 0.00132 \text{ cal/cm s K}$	$k = 3.8 \times 10^{-2} \text{ cal/cm s K}$

(A) An Impermeable Sheet Inserted

The degree of separation is analyzed for $C_f = 0.1$ and $C_f = 0.7$, with the channel thickness ratio κ as a parameter, as shown in Figs. 6 and 7. It is found in these figures that the maximum degree of separation for the $C_f = 0.1$ and $C_f = 0.7$ in double-flow inclined thermal-diffusion columns with an impermeable sheet can be obtained at $\kappa = 0.75$. Although the inclination effect has positive influences on the degree of separation for the device with an impermeable barrier, there exists the best angle of inclination. For $R = 3.0$ and $\sigma = 1.0 \text{ g/hr}$, as shown in Figs. 6 and 7, the best angle is 40° – 50° . It also is shown in Fig. 4 that for $\kappa = 0.75$ and $R = 3.0$ with a specified area, say $A = L \times B = 122 \text{ cm} \times 10.12 \text{ cm}$, the maximum degree of separation decreases as the aspect ratio, L/B , moves away from 3.01. Some numerical values of the improvement performance I are given in Table 4. The separation efficiency improvement can be analyzed for any C_f , κ , and ϕ .

(B) A Permeable Barrier Inserted

The variations of degree of separation and separation efficiency improvement with the feed concentration, angle of inclination, channel thickness ratio, and aspect ratio are presented in Figs. 5, 8, and 9 and Table 5. One may notice in Figs. 8 and 9, and in Table 5 that the maximum degree of separation occurs at $\kappa = 0.75$ and $\phi = 30$ – 40° . It also is shown in Fig. 5 that for $\kappa = 0.75$ with a specified area, the maximum degree of separation decreases as the aspect ratio, L/B , moves away from 3.01.

The separation efficiency improvements, I and I_m , as defined by Eqs. (37) and (38) are shown in Tables 4 and 5. It is shown in Tables 4 and 5 that the separation efficiency improvement of the device with an impermeable sheet



Table 2. Eigenvalues and expansion coefficients for the device with inserting an impermeable sheet; $R = 3.0$, $\sigma = 1.0 \text{ g/hr}$, $k = 0.5$, $C_f = 0.1$.

ϕ	m	λ_e	λ_s	$S_{Ae,m}$	$S_{Be,m}$	$S_{As,m}$	$S_{Bs,m}$	$\Delta(\lambda_{e,1}, \lambda_{s,1})$ (%)	$\Delta(\lambda_{e,1}, \lambda_{s,1})$ (%)
0°	1	-0.79	0.79	-4.28×10^{-3}	9.12×10^{-3}	-9.12×10^{-3}	4.28×10^{-3}	0.400494	0.400562
	2	-10.27	10.27	2.26×10^{-7}	8.20×10^{-8}	-7.92×10^{-8}	-2.28×10^{-7}		
10°	1	-0.79	0.798	-4.37×10^{-3}	10.02×10^{-3}	-9.78×10^{-3}	4.48×10^{-3}	0.4697	0.4698
	2	-10.29	10.29	5.68×10^{-7}	2.21×10^{-7}	-2.18×10^{-7}	-4.78×10^{-7}		
30°	1	-0.79	0.79	-5.22×10^{-3}	8.66×10^{-3}	-8.58×10^{-3}	5.16×10^{-3}	0.5637	0.5639
	2	-10.30	10.30	5.08×10^{-7}	10.09×10^{-8}	-10.5×10^{-8}	-5.07×10^{-7}		
50°	1	-0.79	0.79	-5.53×10^{-3}	7.58×10^{-3}	-7.42×10^{-3}	5.47×10^{-3}	0.6576	0.6578
	2	-10.30	10.30	4.01×10^{-7}	9.72×10^{-8}	-9.62×10^{-8}	-3.98×10^{-7}		
70°	1	-0.79	0.79	-5.78×10^{-3}	7.22×10^{-3}	-7.11×10^{-3}	5.78×10^{-3}	0.7516	0.7518
	2	-10.31	10.31	3.36×10^{-7}	9.30×10^{-8}	-9.02×10^{-8}	-3.38×10^{-7}		



Table 3. Eigenvalues and expansion coefficients for the device with inserting a permeable barrier; $R = 3.0$, $\sigma = 1.0 \text{ g/hr}$, $k = 0.5$, $C_f = 0.1$.

R	m	$\lambda_{\text{Ae},m}$	$\lambda_{\text{Be},m}$	$S_{\text{Ae},m}$	$S_{\text{Be},m}$	$\lambda_{\text{As},m}$	$\lambda_{\text{Bs},m}$	$S_{\text{As},m}$	$S_{\text{Bs},m}$	$\Delta_m(\lambda_{\text{Ae},1}, \lambda_{\text{Be},1}, \lambda_{\text{As},1}, \lambda_{\text{Bs},1}, \lambda_{\text{Ae},2}, \lambda_{\text{Be},2}, \lambda_{\text{As},2}, \lambda_{\text{Bs},2}) (\%)$
0°	1	-9.64	-12.97	9.58×10^{-6}	3.41×10^{-6}	9.64	12.97	3.41×10^{-6}	9.58×10^{-6}	0.764103
	2	-19.64	-27.08	6.47×10^{-11}	2.62×10^{-10}	19.88	27.08	2.62×10^{-10}	6.47×10^{-11}	
10°	1	-9.64	-12.97	9.38×10^{-6}	3.21×10^{-6}	9.64	12.97	3.21×10^{-6}	9.38×10^{-6}	0.8548
	2	-19.88	-27.08	6.27×10^{-11}	2.42×10^{-10}	19.88	27.08	2.42×10^{-10}	6.27×10^{-11}	
30°	1	-9.65	-12.96	-8.26×10^{-6}	-6.61×10^{-6}	9.65	12.96	-6.61×10^{-6}	-8.26×10^{-6}	1.0255
	2	-19.88	-27.08	-5.53×10^{-11}	-4.52×10^{-10}	19.88	27.08	-4.52×10^{-10}	-5.53×10^{-11}	
50°	1	-9.66	-12.95	9.38×10^{-6}	10.13×10^{-6}	9.66	12.95	10.13×10^{-6}	9.38×10^{-6}	1.1966
	2	-19.89	-27.09	6.25×10^{-11}	7.22×10^{-10}	19.89	27.09	7.22×10^{-10}	6.25×10^{-11}	
70°	1	-9.67	-12.93	-2.05×10^{-6}	-6.62×10^{-6}	9.67	12.93	-6.62×10^{-6}	-2.05×10^{-6}	1.3678
	2	-19.89	-27.09	-7.28×10^{-11}	-4.52×10^{-10}	19.89	27.09	-4.52×10^{-10}	-7.28×10^{-11}	



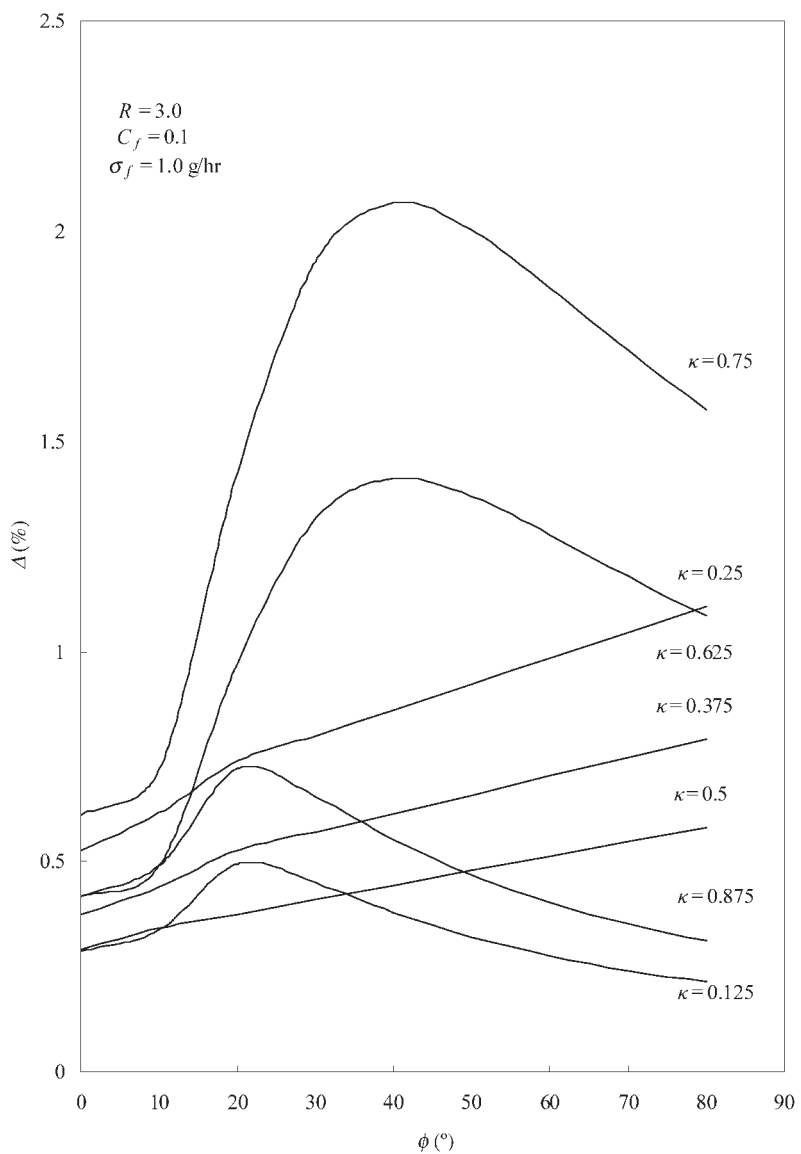


Figure 6. Effect of inclined angle on the degree of separation with sheet position as a parameter; $C_f = 0.1$, $\sigma = 1.0$ g/hr, $R = 3.0$.



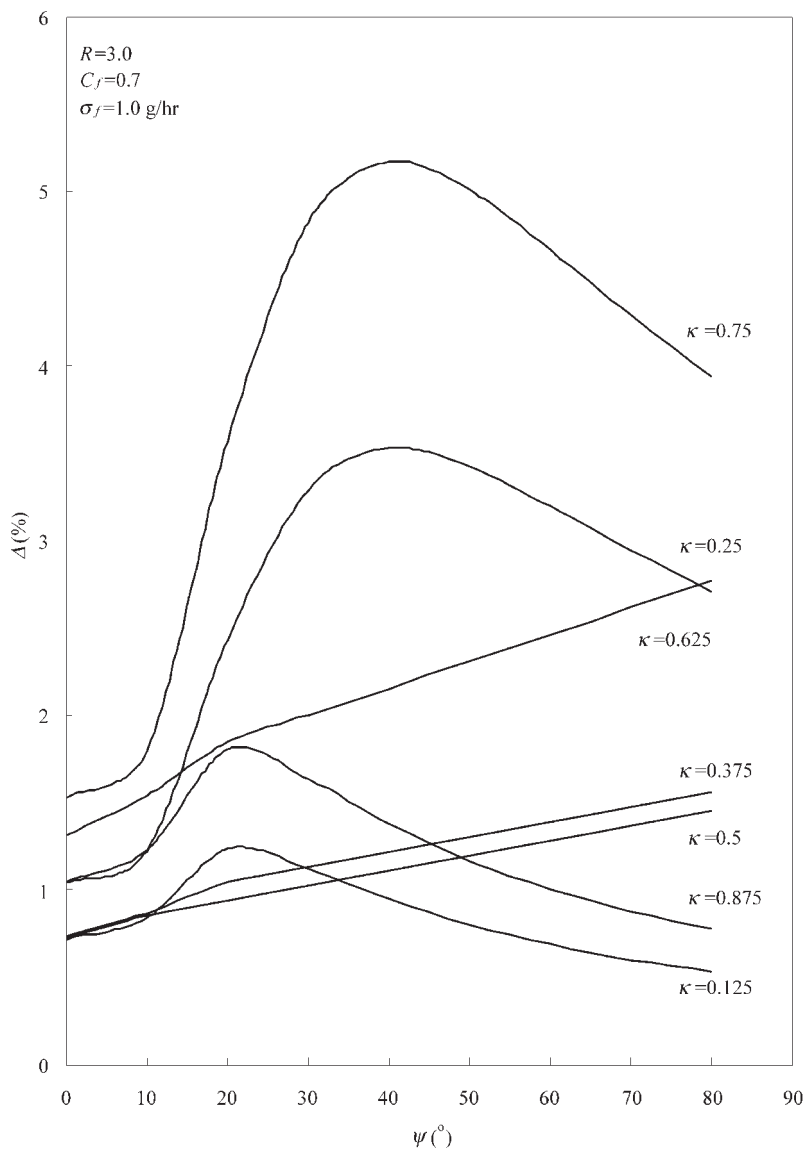


Figure 7. Effect of inclined angle on the degree of separation with sheet position as a parameter; $C_f = 0.7$, $\sigma = 1.0$ g/hr, $R = 3.0$.



Table 4. The separation efficiency improvement for the device of inserting an impermeable sheet with the angles of inclination, channel thickness ratio, feed fraction, and recycle ratio as parameters.

$\sigma = 1.0 \text{ g/hr}$									
$C_f = 0.1$									
ϕ	$R = 1.0$			$R = 3.0$			$R = 1.0$		
	$\kappa = 1/4$	$\kappa = 1/2$	$\kappa = 3/4$	$\kappa = 1/4$	$\kappa = 1/2$	$\kappa = 3/4$	$\kappa = 1/4$	$\kappa = 1/2$	$\kappa = 3/4$
10°	147.54	72.95	263.01	111.65	47.87	210.37	71.91	20.11	152.09
20°	190.37	102.87	325.82	148.26	73.45	264.07	101.66	40.89	195.71
30°	477.16	123.15	746.33	393.47	90.80	623.61	300.83	54.98	487.74
40°	711.29	143.44	1074.97	567.62	108.14	878.57	492.36	69.07	744.89
50°	737.91	163.73	1126.98	616.41	125.49	949.06	481.92	83.16	752.08
60°	712.55	184.02	1088.17	594.73	142.83	915.88	464.30	97.25	725.13
70°	658.44	204.30	1007.07	548.46	160.18	846.54	426.72	111.34	668.81



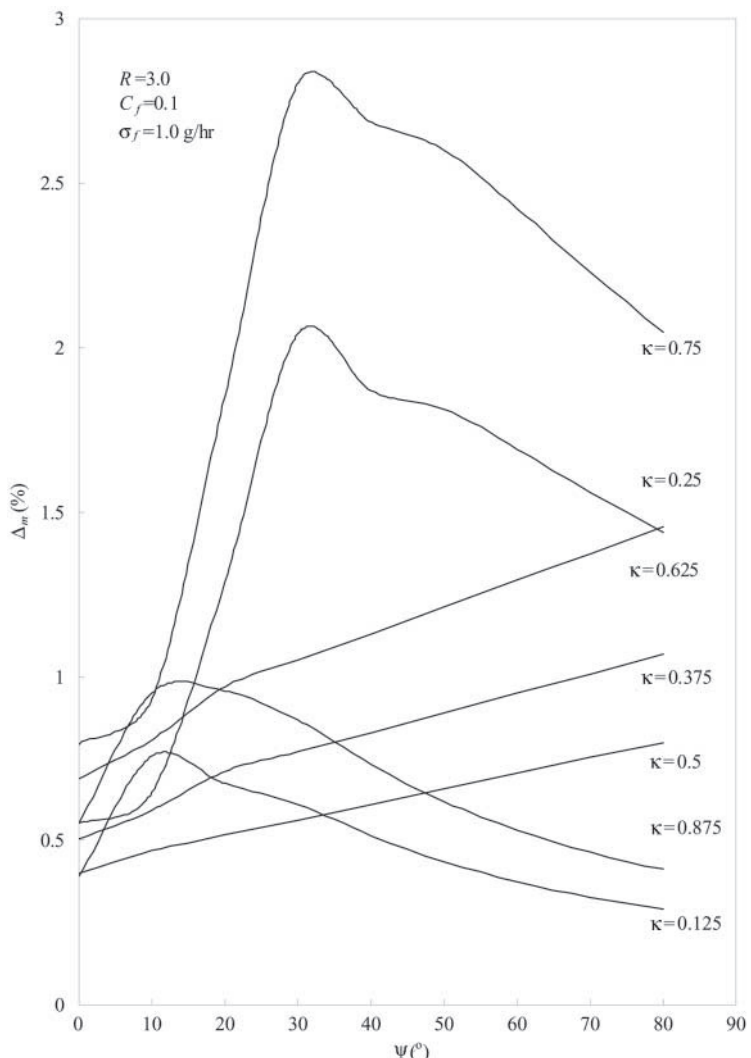


Figure 8. Effect of inclined angle on the degree of separation with barrier position as a parameter; $C_f = 0.1$, $\sigma = 1.0$ g/hr, $R = 3.0$.

inserted increases as ϕ goes away from 40° to 50° . The effects of κ on I and I_m are also presented in Tables 4 and 5. The separation degree improvements, I and I_m , increase as κ goes away from two peaks, say $\kappa = 1/4$ and $\kappa = 3/4$. It is noted that the improvements of the degree of separation, I and I_m , increase when κ goes away from $1/2$, especially for $\kappa > 1/2$, and the separation degree



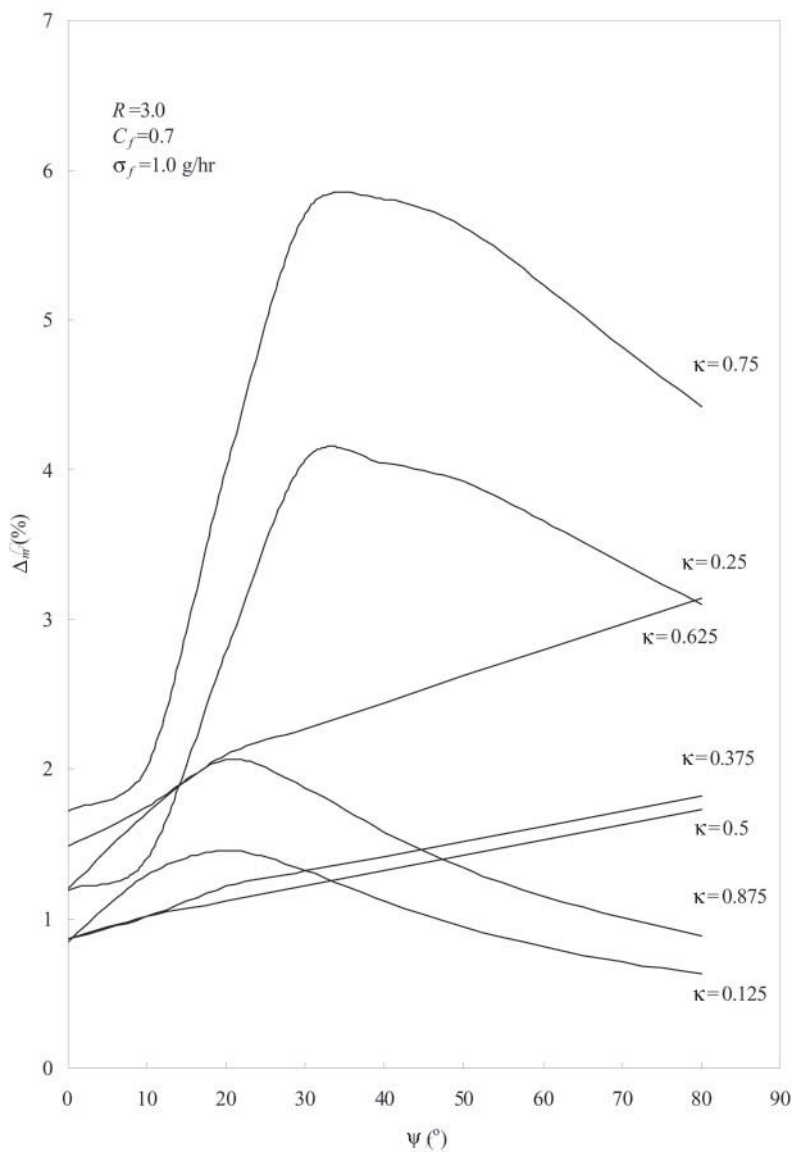


Figure 9. Effect of inclined angle on the degree of separation with barrier position as a parameter; $C_f = 0.7$, $\sigma = 1.0 \text{ g/hr}$, $R = 3.0$.



Table 5. The separation efficiency improvement for the device of inserting a permeable barrier with the angles of inclination, channel thickness ratio, feed fraction, and recycle ratio as parameters.

ϕ	$\sigma = 1.0 \text{ g/hr}$							
	$C_f = 0.7$				$C_f = 0.1$			
	$R = 1.0$		$R = 3.0$		$R = 1.0$		$R = 3.0$	
$\kappa = 1/4$	$\kappa = 1/2$	$\kappa = 3/4$	$\kappa = 1/4$	$\kappa = 3/4$	$\kappa = 1/4$	$\kappa = 3/4$	$\kappa = 1/4$	$\kappa = 3/4$
10°	183.38	105.46	307.72	142.29	75.66	248.60	104.30	48.12
20°	232.41	141.00	378.27	184.21	106.06	308.92	139.64	73.75
30°	560.73	165.10	850.58	464.92	126.66	712.75	376.34	91.13
40°	793.90	189.20	1185.50	725.17	147.27	1059.99	611.204	108.50
50°	859.23	213.30	1278.11	720.13	167.87	1078.28	591.54	125.88
60°	830.19	237.41	1234.52	695.31	188.48	1041.02	570.60	143.25
70°	768.25	261.51	1143.43	642.35	209.09	963.13	525.95	160.63



improvements rise with increasing the reflux ratio but fall with increasing the feed fraction.

CONCLUSIONS

Separation efficiency of double-flow thermal-diffusion columns with the insertion of an impermeable sheet or a permeable barrier has been investigated and solved analytically by using the orthogonal expansion technique with eigenfunction expanded in terms of an extended power series. The approximation solution in the inclined Clusius–Dickel column was derived by the transport equation, Eq. (1), and the analytical solution in this study was found from Eq. (35) [or Eq. (36)]. For an illustration, the design parameters ($W = 0.08$, $\phi = 0^\circ$, and $\kappa = 0.9999 \approx 1$) and operating parameters ($\sigma = 1.0 \text{ g/hr}$ and $R = 0$) were used to check the degree of separation with feed fraction concentration as a parameter for both analytical and approximation solutions, and the comparisons of those two solutions were made and presented in Table 6. The approximation solutions were validated from our previous work.^[29] It is found from Table 6 that the theoretical solutions conform pretty well with the approximation solutions.

The influences of aspect ratio and inclined angle on the best performance of such devices are investigated by keeping a constant plate surface area, which implies a constant equipment cost. The optimal aspect ratio is $L/B = 61 \text{ cm}/20.24 \text{ cm} = 3.01$, and the optimal angle is $\phi = 30^\circ\text{--}40^\circ$ and $40^\circ\text{--}50^\circ$ with an impermeable sheet inserted and a permeable barrier inserted, respectively. The analytical results, as shown in Figs. 6–9 indicate that the separation efficiency enhancement occurs for the device with a permeable

Table 6. Comparisons of the degree of separation between the analytical and approximation solutions in the inclined Clusius–Dickel column with feed fraction concentration as a parameter.

C_f	Δ (%)	
	Approximation solutions obtained from Eq. (1)	Analytical solution obtained from Eq. (35) [or Eq. (36)]
0.1	0.341	0.345
0.3	0.590	0.591
0.5	0.635	0.635
0.7	0.536	0.537
0.9	0.194	0.197



barrier. While designing such devices with an impermeable sheet and a permeable barrier inserted, proper angle of inclination, and ratio of channel thickness can be determined technically with economical feasibility. Moreover, the position of the impermeable sheet and permeable barrier has significant influence on the mass transfer behavior in double-pass operations. It is clear from the results that the maximum separation efficiency improvement can be obtained at certain insertion locations.

NOMENCLATURE

B	column width (cm)
C	fraction concentration of D_2O in H_2O -HDO- D_2O system (—)
D	ordinary diffusion coefficient (cm^2/s)
d_{mn}	coefficient in the eigenfunction F_m for region A (—)
e_{mn}	coefficient in the eigenfunction F_m for region B (—)
F_m	eigenfunction associated with eigen value λ_m (—)
$\hat{C}C$	pseudoproduct form of concentration for D_2O defined by Eq. (4) (—)
F_e, F_s	appropriate values of $\hat{C}C$ in enriching section, in stripping section (—)
f_1, f_2, f_3	constants defined in the velocity distribution of region A (—)
G_m	function defined during the use of orthogonal expansion method (—)
g	gravitational acceleration (cm/s^2)
g_1, g_2, g_3	constants defined in the velocity distribution of region B (—)
H	transport coefficient defined by Eq. (2) (g/s)
I_m, I	improvement of the degree of separation defined by Eqs. (37) and (38) (—)
J_x, J_z	mass flux of component 1 in the x and z direction ($g/cm^2 s$)
K	transport coefficient defined by Eq. (2) ($g/s cm$)
K_{eq}	mass-fraction equilibrium constant of H_2O -HDO- D_2O system (—)
k, k_f	thermal conductivity of the barrier and the fluid, respectively ($cal/cm s K$)
L	one-half of column length (cm)
L'	dimensionless coordinate by Eq. (3) (—)
q_m	ratio of expansion coefficients associated with eigenvalue λ_m (—)
R	reflux ratio at both ends of the column (—)
S_m	expansion coefficient associated with eigenvalue λ_m (—)
\tilde{T}	reference temperature evaluated by Eq. (9) (K)



T_1, T_2	temperatures of the cold and hot plates, respectively (K)
ΔT	difference in temperature of hot and cold surfaces (K)
V	velocity distribution of fluid in the vertical direction (cm/s)
W	thickness of the region (cm)
x	coordinate in the horizontal direction (cm)
z	coordinate in the vertical direction (cm)

Greek Symbols

α	thermal diffusion constant for D_2O in $\text{H}_2\text{O}-\text{HDO}-\text{D}_2\text{O}$ system (—)
β	$(\partial\rho/\partial T)$ evaluated at reference temperature (g/cm ³ K)
Δ	degree of separation, $C_B - C_T$ (—)
Δ_e, Δ_s	$C_B - C_F, C_F - C_T$ (—)
δ	thickness of the barrier (cm)
ε	permeability of the barrier (—)
ζ	dimensionless coordinate in the vertical direction, defined by Eq. (9) (—)
η	dimensionless coordinate in the horizontal direction, defined by Eq. (9) (—)
ϕ	angle of inclination of column plate from the vertical (°)
λ_m	eigenvalue (—)
μ	viscosity of fluid (g/cm s)
ρ	density of fluid (g/cm ³)
σ	mass flow rate of top or bottom product (g/hr)
σ'	dimensionless mass flow rate defined by Eq. (3) (—)
κ	the position of an impermeable sheet or a permeable barrier

Subscripts

A	in the channel A
B	in the channel B
b	at end of the enriching section
e	in the enriching section
f	of feed stream
t	C at end of stripping section
s	in the stripping section

ACKNOWLEDGMENT

The authors wish to thank the National Science Council of the Republic of China for its financial support.



REFERENCES

1. Enskog, D. A generalization of maxwell's second kinetic gas theory. *Physik. Z.* **1991**, *12*, 56–68.
2. Chapman, S.; Dootson, F.W. Thermal diffusion. *Phil. Mag.* **1917**, *33*, 248–256.
3. Clusius, K.; Dickel, G. Neues verfahren zur gasentmischung und isotopentrennung. *Naturwissenschaften*. **1938**, *26*, 546–552.
4. Clusius, K.; Dickel, G. Grundlagen eines neuen verfahrens zur gasentmischung und isotopentrennung durch thermodiffusion. *Z. Phys. Chem.* **1939**, *B44*, 397–450.
5. Furry, W.H.; Jones, R.C.; Onsager, L. On the theory of isotope separation by thermal diffusion. *Phys. Rev.* **1939**, *55*, 1083–1095.
6. Jones, R.C.; Furry, W.H. The separation of isotopes by thermal diffusion. *Rev. Mod. Phys.* **1946**, *18*, 151–224.
7. Yeh, H.M.; Yang, S.C. The enrichment of heavy water in a batch-type thermal diffusion column for whole range of concentration. *Chem. Eng. Sci.* **1984**, *39*, 1277–1282.
8. Yeh, H.M.; Yang, S.C. The enrichment of heavy water in a continuous flow thermal diffusion column. *Sep. Sci. Technol.* **1985**, *20*, 101–114.
9. Yeh, H.M. Enrichment of heavy water by thermal diffusion. *Chem. Eng. Comm.* **1998**, *167*, 167–179.
10. Power, J.E.; Wilke, C.R. Separation in liquid by thermal diffusion. *AIChE J.* **1957**, *3*, 213–217.
11. Washall, T.A.; Molpolder, F.W. Improving the separation efficiency of liquid thermal diffusion columns. *IEC Proc. Dec. Dev.* **1962**, *1*, 26–28.
12. Chueh, P.L.; Yeh, H.M. Thermal diffusion in a flat-plate column inclined for improved performance. *AIChE J.* **1967**, *13*, 37–41.
13. Yeh, H.M.; Ward, H.C. The improvement in separation of concentric tube thermal diffusion columns. *Chem. Eng. Sci.* **1971**, *26*, 937–947.
14. Ramser, J.H. Theory of thermal diffusion under linear fluid shear. *Ind. Eng. Chem.* **1957**, *49*, 155–158.
15. Yeh, H.M.; Tsai, C.S. The improvement in separation of continuous-type thermal diffusion columns with walls set in parallel opposite motion. *Chem. Eng. Sci.* **1972**, *27*, 2065–2071.
16. Sullivan, L.J.; Ruppel, T.C.; Willingham, C.B. Rotary and packed thermal diffusion fractionating columns for liquids. *Ind. Eng. Chem.* **1955**, *47*, 208–212.
17. Yeh, H.M.; Chen, S.M. A study on the separation efficiency of rotary thermal diffusion columns. *Chem. Eng. Sci.* **1973**, *28*, 1083–1088.



18. Yeh, H.M.; Tsai, S.W. Improvement in separation of concentric-tube thermal diffusion columns with viscous heat generation under consideration of the curvature effect. *Sep. Sci. Technol.* **1981**, *16*, 63–73.
19. Yeh, H.M.; Tsai, S.W. Separation efficiency of rotary thermal diffusion columns with inner tube cooled and outer tube heated. *Sep. Sci. Technol.* **1982**, *17*, 1075–1083.
20. Lorenz, M.; Emery, A.H., Jr. The packed thermal diffusion column. *Chem. Eng. Sci.* **1959**, *11*, 16–23.
21. Yeh, H.M.; Chu, T.Y. A study of the separation efficiency of continuous-type packed thermal diffusion columns. *Chem. Eng. Sci.* **1974**, *29*, 1421–1425.
22. Yeh, H.M.; Ho, F.K. A study of the separation efficiency of wired thermal diffusion columns with tubes rotated in opposite directions. *Chem. Eng. Sci.* **1975**, *30*, 1381–1385.
23. Yeh, H.M.; Tsai, C.W. A study of the separation efficiency of rotated concentric-tube thermal diffusion columns with helical plane inserted as a spacer in the annulus. *J. Chem. Eng. Japan.* **1981**, *14*, 90–97.
24. Yeh, H.M.; Tsai, C.W.; Lin, C.S. A study of the separation efficiency in thermal diffusion columns with a permeable vertical barrier. *AIChE J.* **1986**, *32*, 971–980.
25. Yeh, H.M.; Tsai, C.W.; Chen, W.H. Improvement of separation efficiency in the continuous-type horizontal thermal-diffusion columns with permeable barriers between the plates. *Can. J. Chem. Eng.* **1986**, *64*, 687–694.
26. Tsai, C.W.; Yeh, H.M. A study of the separation efficiency of the continuous thermal diffusion column with an impermeable barrier between plates. *J. Chem. Eng. Japan.* **1986**, *19*, 548–553.
27. Ho, C.D.; Yeh, H.M.; Chiang, S.C. Mass-transfer enhancement in double-pass mass exchangers with external refluxes. *Ind. Eng. Chem. Res.* **2001**, *40*, 5839–5846.
28. Ho, C.D.; Yeh, H.M.; Chiang, S.C. A study of mass transfer efficiency in a parallel-plate channel with external refluxes. *Chem. Eng. J.* **2002**, *85*, 207–214.
29. Ho, C.D.; Yeh, H.M.; Guo, J.J. An analytical study on the enrichment of heavy water in the continuous thermal diffusion column with external refluxes. *Sep. Sci. Technol.* **2002**, *37*, 687–694.
30. Treacy, J.C.; Rich, R.E. Barrier system in thermal diffusion columns. *Ind. Eng. Chem.* **1955**, *47*, 1544.
31. Singh, S.N. The determination of eigen-functions of a certain sturm-liouville equation and its application to problems of heat-transfer. *Appl. Sci. Res. Section A.* **1958**, *32*, 237–250.



32. Brown, G.M. Heat or mass transfer in a fluid in laminar flow in a circular or flat conduit. *AIChE J.* **1960**, *6*, 179–183.
33. Tsai, S.W.; Yeh, H.M. A study of the separation efficiency in horizontal thermal diffusion columns with external refluxes. *Can. J. Chem. Eng.* **1985**, *63*, 406–411.
34. Yeh, H.M.; Tsai, S.W.; Cheng, T.W. A study of the graetz problem in concentric-tube continuous-contact countercurrent separation processes with recycles at both ends. *Sep. Sci. Technol.* **1986**, *21*, 403–419.
35. Ebadian, M.A.; Zhang, H.Y. An exact solution of extended Graetz problem with axial heat conduction. *Int. J. Heat Mass Transfer.* **1989**, *32*, 1709–1717.
36. Standen, A. *Encyclopedia of Chemical Technology*, 3rd Ed.; Wiley: New York, 1978; Vol. 7; 549.

Received June 2003

Revised September 2003



Request Permission or Order Reprints Instantly!

Interested in copying and sharing this article? In most cases, U.S. Copyright Law requires that you get permission from the article's rightsholder before using copyrighted content.

All information and materials found in this article, including but not limited to text, trademarks, patents, logos, graphics and images (the "Materials"), are the copyrighted works and other forms of intellectual property of Marcel Dekker, Inc., or its licensors. All rights not expressly granted are reserved.

Get permission to lawfully reproduce and distribute the Materials or order reprints quickly and painlessly. Simply click on the "Request Permission/Order Reprints" link below and follow the instructions. Visit the [U.S. Copyright Office](#) for information on Fair Use limitations of U.S. copyright law. Please refer to The Association of American Publishers' (AAP) website for guidelines on [Fair Use in the Classroom](#).

The Materials are for your personal use only and cannot be reformatted, reposted, resold or distributed by electronic means or otherwise without permission from Marcel Dekker, Inc. Marcel Dekker, Inc. grants you the limited right to display the Materials only on your personal computer or personal wireless device, and to copy and download single copies of such Materials provided that any copyright, trademark or other notice appearing on such Materials is also retained by, displayed, copied or downloaded as part of the Materials and is not removed or obscured, and provided you do not edit, modify, alter or enhance the Materials. Please refer to our [Website User Agreement](#) for more details.

Request Permission/Order Reprints

Reprints of this article can also be ordered at

<http://www.dekker.com/servlet/product/DOI/101081SS120028565>